Spin-reorientation transition in thin films studied by the component-resolved Kerr effect

H. F. Ding, S. Pütter,* H. P. Oepen,*,† and J. Kirschner
Max-Planck Institut für Mikrostrukturphysik, Weinberg 2, 06120 Halle, Germany
(Received 24 July 2000; published 14 March 2001)

We present a method to separate the longitudinal, polar, and equatorial magnetization components that may contribute to a mixed magneto-optical Kerr-effect signal and demonstrate how the spin-reorientation transition (SRT) can be investigated by means of simple Kerr magnetometry. In a Co/Au(111) film with thickness within the SRT region we find hysteresis loops with nonvanishing remanence in all three components when a field is applied within the film plane. A vertical field, however, drives the same film into a single domain state exhibiting full remanence. The fact that remanence is found in all magnetization components, and full remanence is obtained in a vertical field, rules out that the transition proceeds via a state of canting of magnetization and indicates that it proceeds via a state of coexisting phases.

DOI: 10.1103/PhysRevB.63.134425 PACS number(s): 75.70.Ak, 78.20.Ls, 33.55.Fi, 78.20.Jq

I. INTRODUCTION

Conventional methods for obtaining magnetic hysteresis loops, e.g., vibrating sample magnetometry and superconducting quantum interference device susceptometry are commonly used to detect a single component of magnetization parallel to the direction of the external field. A single hysteresis curve obtained with these methods, however, provides only a limited amount of information. Additional information can be produced by rotating the sample in an applied field.[1] A more fundamental method for investigating the magnetization process entails measuring the three components of the magnetization. Some work along this line demonstrated its power 40 years ago. The instruments, however, were rather complex to construct.[2,3]

The magneto-optical Kerr effect (MOKE) has become an important technique for the investigation of surface and ultrathin-film magnetism.[4–6] It has been successfully applied to measure the two orthogonal in-plane components of the magnetization by means of an in-plane vectorial MOKE technique.[7–11] This technique was also used to identify the orientation of in-plane domains in Kerr microscopy.[9,10] Yang and Scheinfein suggested measuring the pure polar signal in a normal-incidence geometry.[12] It appears possible to obtain the individual magnetization components by applying these methods. The very existence of a polar signal, however, prevents the correct measurement of the in-plane components due to the fact that these signals are suppressed by the much stronger polar signal. The mixing of polar and longitudinal signals has been qualitatively discussed in the literature.[13] Berger and Pufall presented a promising technique, i.e., generalized magneto-optical ellipsometry,[14] which allows to determine the orientation of the in-plane magnetization. The authors pointed out that the method is also useful to separate the mixed Kerr signal of out-of-plane and in-plane magnetization. This method, however, is quite involved.

A new method of separating the longitudinal and polar Kerr signal was presented recently.[15] In the present paper this technique is expanded to obtain the information of all three orthogonal magnetization components [three dimensional (3D) MOKE]. We use this method to study the spin-reorientation transition in Co films on Au(111).

In Co/Au(111) a thickness-dependent spin reorientation has been found.[16,17] The competition between surface anisotropy and magnetostatic energy forces the magnetization to flip from perpendicular to in-plane orientation with increasing thickness. The magnetization follows the sweep of an external field applied along the easy axis when the thickness is below or beyond the spin-reorientation transition. Within the spin-reorientation transition the magnetization orientation in a field is still unclear and the subject of ongoing debate. By means of the 3D-MOKE technique we can identify nonvanishing signals in all three components within the thickness span of the SRT when the field is in plane. Applying a field in the vertical direction drives the film into a single domain state with full remanence. This finding indicates that the spin-reorientation transition of Co/Au(111) proceeds via a state of coexisting phases, not via a state of continuous magnetization canting.

In the next section we will summarize the principle of the method and give a detailed description of the experimental verification in the third section. Hysteresis loops obtained with films at three representative thicknesses, i.e., below, beyond, and within the SRT will be discussed in the fourth section.

II. PRINCIPLE

In the framework of the linear Kerr effect, MOKE is classified with respect to the orientation of the magnetization and the light-scattering plane. In the polar Kerr effect the magnetization is normal to the reflecting surface. In the longitudinal/transverse Kerr effect the magnetization is parallel to the sample surface and within/perpendicular to the light-scattering plane, respectively. If the magnetization is oriented in an arbitrary direction the Kerr signal can, in principle, be split into these three basic configurations.

It should be pointed out that the different MOKE geometries are not related to the direction of the applied magnetic field. Particularly in the magnetization reversal process the magnetization will not be strictly fixed to the field direction or along the easy axis. In such a situation, the Kerr signal is a mixture of different Kerr effects. Usually, the mixed Kerr signal gives very complicated hysteresis loops due to the

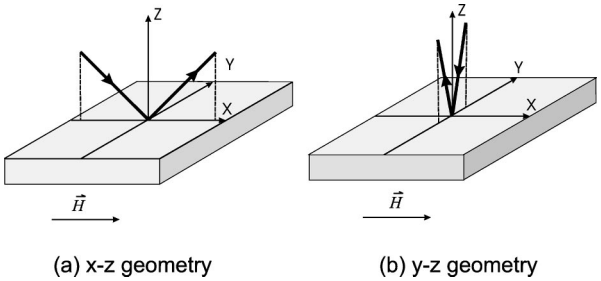

FIG. 1. Experimental setup. (a) The angle of incidence is 45°. The scattering plane is spanned by the direction of the magnetic field (x axis) and the surface normal (z axis). (b) The plane of incidence is perpendicular to the field direction (angle of incidence 9°).

different strength of the individual contributions.[13,15,18–21] The best way to obtain the pure components along different directions is to select a geometry where one component does not contribute and separate the remaining components. The third component can be achieved through a second similar measurement.

In a simplified classical model the linear Kerr effect can be understood as the change of the electric-field vector of the light due to Lorentz force caused by the magnetization of the material.[19] Hence, no Kerr signal is found when the magnetization is parallel to the electric field of the light. This situation appears for the transverse Kerr effect with *s*-polarized light. Vice versa, it means that by using *s*-polarized light the transverse Kerr effect can be eliminated and only polar and longitudinal components remain, which can be separated in the following way.

Recently, a procedure that can be used to separate the longitudinal and polar Kerr signals has been presented.[15] As the polar Kerr signal is an even function and the longitudinal signal is an odd function of the incident angle, the two contributions can be separated. When *s*-polarized light is impinging under a positive angle,[22] the sum of polar and longitudinal contributions is measured; while reversing the optical geometry with respect to the surface normal the difference of both is obtained, i.e.,

$$\varepsilon^{\pm\theta} = \varepsilon^{P} \pm \varepsilon^{L}, \tag{1}$$

with $\varepsilon^{\pm\theta}$ the Kerr ellipticities for the respective angles of incidence, and ε^{P} and ε^{L} the ellipticities for the polar and longitudinal Kerr effects. Hence, by two measurements in reversed geometries one can separate the longitudinal and polar Kerr signals. We will explain in the following how the third component of the magnetization can be determined.

For the sake of simplicity we introduce a frame of reference. As shown in Fig. 1, we define the surface normal as the z direction. The x and y directions are lying within the film plane. The field is acting along the x axis. When the xz plane is the light-scattering plane (''x-z geometry'') the magnetization component along the y direction (M_y) will not contribute to the Kerr signal when using *s*-polarized light. Hence, this MOKE setup is only sensitive to M_x and M_z, which causes a longitudinal and polar signal, respectively. The signals can be separated by two measurements in reversed geometries as explained above.

Rotating the MOKE optics by 90° about the surface normal (alternatively one may rotate the sample and the applied field by 90°) the yz plane becomes the scattering plane while the field is still oriented along the x direction [''y-z geometry'' in Fig. 1(b)]. In this geometry the MOKE setup is sensitive to M_y and M_z giving a longitudinal and polar signal, respectively. Applying the same technique the component M_y is obtained while the component M_z is measured redundantly. Thus, by using four different geometries, related to each other by mirror symmetry and a 90° rotation, all three components are obtained. The redundant measurement of M_z serves as an important consistency check.

III. EXPERIMENTS

The Co films were grown on a Au(111) single crystal under UHV conditions by means of *e*-beam evaporation at room temperature. Utilizing medium-energy electron-diffraction intensity oscillations the evaporation rate was calibrated with an error margin of 5%. The typical rate of deposition was 0.4 ML/min. The gold crystal was cleaned by 1-kV-Ar ion etching at a 30° angle of incidence and annealing at 900 K for half an hour. The $23\times\sqrt{3}$ reconstruction of Au (Refs. 23,24) was clearly seen in the low-energy electron-diffraction pattern. After growth the films have been annealed at 510 K for 10 min in order to stabilize the magnetic properties, stop the Au diffusion, and smooth the sample surface.[25] Co films with different thicknesses were grown to cover the full range of the spin-reorientation transition. We will discuss in the following the magnetic properties of three representative thicknesses, i.e., below, within, and beyond the spin-reorientation transition.

For the measurement of the magnetic properties, we use two optical setups with perpendicular scattering planes as shown in Fig. 1. The external field was applied along the x direction.[26] The ''x-z geometry'' is sensitive to M_x and M_z while the other one, i.e., ''y-z geometry'' is sensitive to M_y and M_z. Due to experimental restrictions the angle of incidence for the ''x-z geometry'' is 45° and for ''y-z geometry'' it is 9°. In a third MOKE geometry the polar Kerr effect is obtained under 15° in a vertical field along z.

S-polarized light was used in all MOKE setups to minimize the signals caused by the transverse Kerr effect. Quarter-wavelength plates have been incorporated in the optics to minimize the window effects and thus increase the sensitivity.[27] Due to the 90° phase shift induced by the quarter-wavelength plate the Kerr ellipticity instead of the Kerr rotation is obtained.[28]

The laser spots of both MOKE setups were kept on the same position (uncertainty was less than 20% of the laser-spot diameter) on the sample to reduce the uncertainty of the alignment when reversing geometry, i.e., interchanging the light source and the detector. The positions where the light passes through the windows have been marked. The optics, i.e., laser and polarizer as well as the analyzer components, were fixed to two rigid supports that were tightly clamped to the windows of the UHV chamber. The combination of

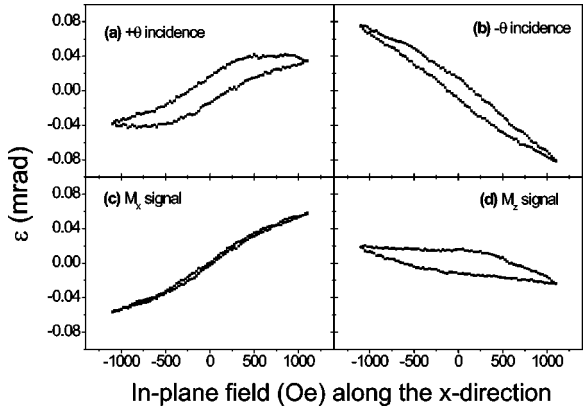

FIG. 2. Hysteresis loops at a thickness just before the spin-reorientation transition (5.0 ± 0.3 ML) obtained in the ''*x*-*z* geometry.'' (a) and (b) are hysteresis loops obtained at a $\pm45°$ angle of incidence. (c) and (d) are the pure components along the *x* and *z* directions. They are deconvoluted from (a) and (b).

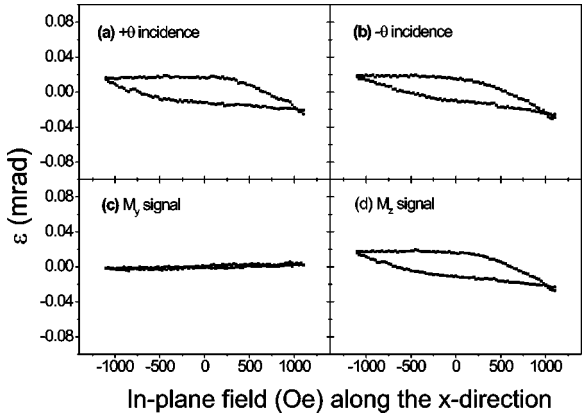

FIG. 3. Hysteresis loops obtained in the ''*y*-*z* geometry'' with the same film as in Fig. 2. The hysteresis loops in (a) and (b) are obtained at a $\pm9°$ angle of incidence. (c) and (d) are the pure components along the *y* and *z* directions. They are deconvoluted from (a) and (b).

marking the positions on the windows and the rigid support for the optics reduces the uncertainty in the angle of incidence to less than 1° on reversing the geometry. As the sensitivity of the polar and longitudinal Kerr effect is only weakly dependent on the angle around 45° small changes in the angle of incidence can be neglected in the ''*x*-*z* geometry.''[20]

In the ''*y*-*z* geometry,'' a larger uncertainty of the longitudinal signal is expected due to the uncertainty of the angle on reversing the geometry, as at 9° a stronger angle dependence of the Kerr signal is effective. Utilizing the formulas given by Zak and co-workers,[20] the Voigt constant from Ref. 29, and tabulated values for the index of refraction[30] we can estimate an uncertainty of about 10% for the longitudinal signal for a 1° deviation of the angle of incidence. Small changes in the angle of incidence must not be considered for the polar signal since the sensitivity is constant around 9°.

Due to the different angles of incidence we cannot directly compare the magnitude of the longitudinal signals. We have calculated the angle-dependent Kerr ellipticity of the longitudinal signal using the method mentioned above. We find that the sensitivity of the longitudinal signal at 45° is four times larger than that at 9°. As the Kerr signal is linear with the film thickness in the ultrathin-film approximation,[20] we use this ratio to compare the longitudinal signals obtained in both MOKE setups.[31]

IV. EXPERIMENTAL RESULTS

Figs. 2(a) and (b) show the hysteresis loops obtained in the ''*x*-*z* geometry'' for opposite angles of incidence. The thickness of 5.0 ± 0.3 ML is chosen just below the SRT. The magnetic field was applied along the *x* axis. Using the procedure mentioned at the beginning, the longitudinal (M_x) and polar (M_z) signal can be extracted [see Figs. 2(c) and (d)]. M_x shows a hard axis loop with almost no remanence and M_z reveals a hysteresis that is apparently not saturated.

Hysteresis loops taken with the MOKE setup in the *yz* plane in the same field are plotted in Figs. 3(a) and (b). The deconvoluted longitudinal signal (M_y) and polar signal (M_z) are shown in Figs. 3(c) and (d). It is important to note that the polar signals in both MOKE setups are the same although the angles of incidence are different [see Figs. 2(d) and 3(d)]. It means that the sensitivity of the polar Kerr effect is almost constant within that range of angles. This also gives a check of the accuracy of our experimental method. The signal in the *y* direction is very small (below 4 μrad). At the thickness under investigation the magnetic easy axis is perpendicular to the film plane. When the external field is applied along the *x* direction the magnetization is slightly tilted into the field direction. No torque is acting on the magnetization along the *y* direction and no signal appears.

The polar loop shown in Fig. 4(d) was obtained by applying the field in the vertical direction. It exhibits a squarelike

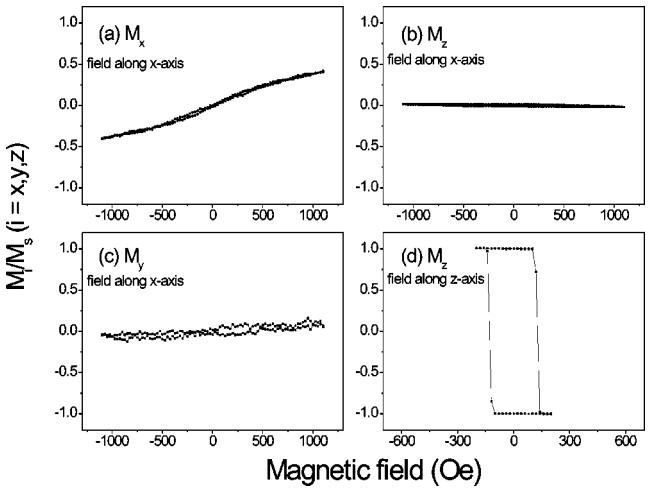

FIG. 4. (a)–(c) are the normalized magnetization components calculated with the data of Figs. 2 and 3. We have used a scaling factor of 8.4 ± 0.5 for the polar-versus-longitudinal Kerr sensitivity at an angle of incidence of 45°, and a factor of 4 ± 0.4 for the longitudinal Kerr sensitivity at the two angles of $\pm45°$ and $\pm9°$. (d) is the hysteresis loop obtained in a vertical field with the same film. The angle of incidence is 15°.

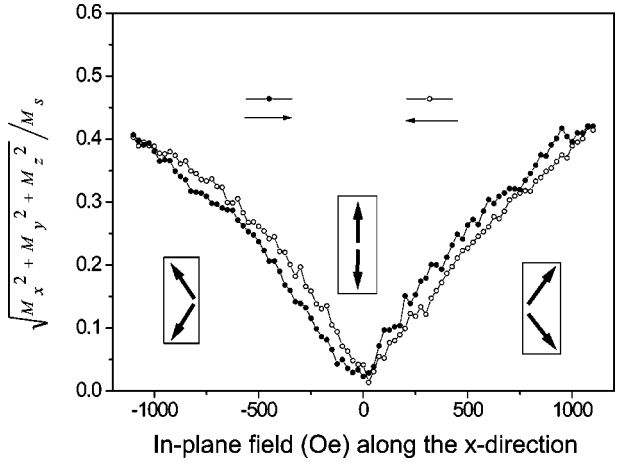

FIG. 5. The value of the magnetization calculated from the individual components in Fig. 4. The thinner arrows in the figures indicate the field scanning direction. The insets give a sketch of the proposed magnetic domain configuration.

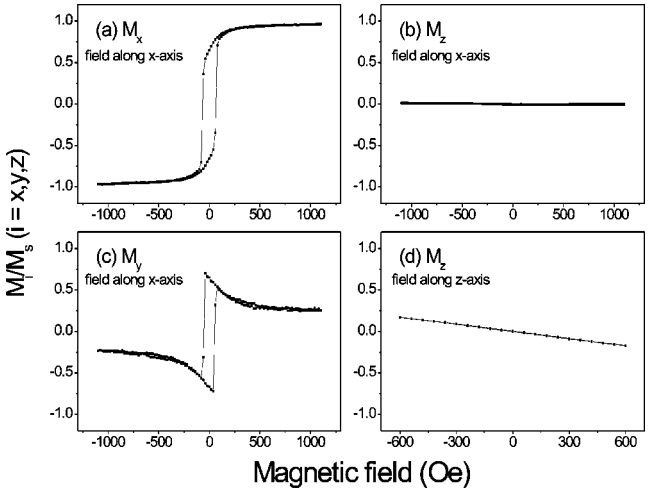

FIG. 6. (a)–(c) are the normalized magnetization components along the different directions deconvoluted from the data obtained at a thickness beyond the spin-reorientation transition (6.1 ± 0.3 ML). The scaling factors are the same as in Fig. 4. Fig. 6(d) is the hysteresis loop obtained with the same film in a vertical field.

easy axis loop with a small coercivity (about 125 Oe), which shows the easy axis to be perpendicular to the film plane. The signal in saturation is 50 times larger than the polar signal obtained in the in-plane field [Fig. 2(d)].

We have investigated the thickness dependence of the longitudinal signal in saturation for in-plane magnetization. From these data we can extrapolate to the film thickness under investigation. A Kerr ellipticity of 140 ± 5 μrad should be expected for the longitudinal signal in saturation. This value is in close agreement with the calculated value of 139 μrad in the 45° geometry.[15] Taking 140 ± 5 μrad and the polar saturation value 1180 ± 25 μrad we can calculate the relative sensitivities of the longitudinal to the polar signal. The polar signal is a factor of 8.4 ± 0.5 stronger than the longitudinal signal for 5 ML Co/Au and for an angle of incidence of 45°. Combining the theoretical and experimental values for the longitudinal Kerr-effect sensitivities we can estimate the relative sensitivities of the Kerr signals along the different components, i.e., 4:1:34 for $M_x:M_y:M_z$.

In Figs. 4(a)–(c), we have scaled the magnetization curves appropriately. Around 42% of the magnetization is found along the *x* direction in high fields. The signal in the *y* direction slightly increases with the field, which can be caused by a small misorientation of the field that causes the magnetization to tilt slightly towards the *y* direction. A small misalignment of the plane of incidence may also contribute to this signal, as a projection of the *x* component can appear. We have plotted (Fig. 5) the square root of the vectorial sum of the individual components (normalized to 100%) as a function of the field along the *x* direction. In this plot the curves show almost no remanence. The 42% of the M_x signal in high field can be interpreted as the magnetization to be tilted by about 25° away from the normal direction. Conversely that means that 9% of the magnetization signal along the *z* direction should be observed in case of a coherent rotation. In our measurement, however, only a 2% signal is found in the *z* component. Hence, we have to assume that the film is split into domains oppositely magnetized along the vertical direction. Applying a field along the *x* direction causes a tilt of the magnetization, i.e., the magnetizations in both spin-up and spin-down domains tilt towards the *x* direction. So a signal appears in the *x* direction while in the *z* direction the signal is almost balanced by domains with opposite vertical components (*z* components). The 2% signal appearing along the *z* direction can be caused by the misalignment of the magnetic field, which causes slightly unbalanced domain configurations or a small difference in the tilting for spin-up and spin-down domains. The magnetization process can be explained as follows: The film is in a multidomain state with a perpendicular direction of magnetization at zero field. The in-plane field forces the magnetization to tilt into the x axis. In the highest field the magnetization is tilted by 25° with respect to the surface normal.

For a thickness beyond the SRT the hard axis is perpendicular to the film plane [see Fig. 6(d) for a 6.1 ± 0.3-ML film]. When the external field is applied within the film plane, the magnetization reversal should proceed within the film plane [Figs. 6(a)–(c)]. In Fig. 6 the individual components of magnetization in an in-plane field are shown and have been scaled with the sensitivities given above and normalized to 100%. We clearly see that the magnetization along the *x* direction has almost reached saturation, i.e., 98% of the full signal is obtained in high fields. In the *z* direction the signal is less than 1%. The remaining signal is due to the misalignment of the magnetic field. Assuming that the Kerr signal that appears along the *z* direction in the in-plane field is caused by the misalignment of the field, we can estimate the angle of misalignment to be roughly 1°, since only 1% of the magnetization signal in high field is found in the *z* direction. Fig. 7 exhibits the field dependence of the magnetization obtained from the loops in Fig. 6. The value is nearly constant except for two dips around ± 60 Oe. First we would like to discuss the reliability of the observed structures. We have taken two possible mechanisms into consideration that could artificially cause sharp structures, i.e., a shift of data points and the uncertainty of the calibration

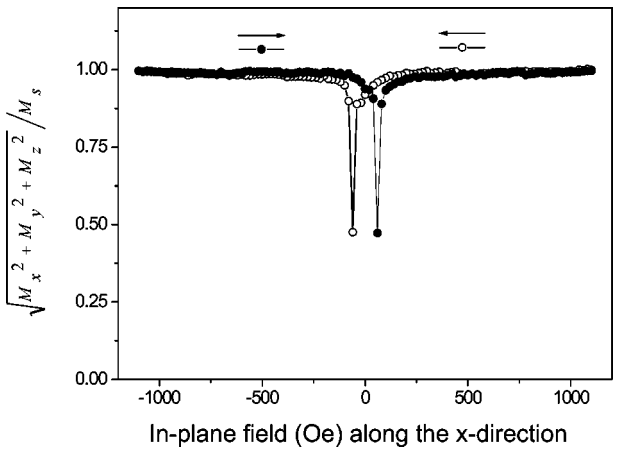

FIG. 7. The normalized value of the magnetization calculated from the individual components in Fig. 6.

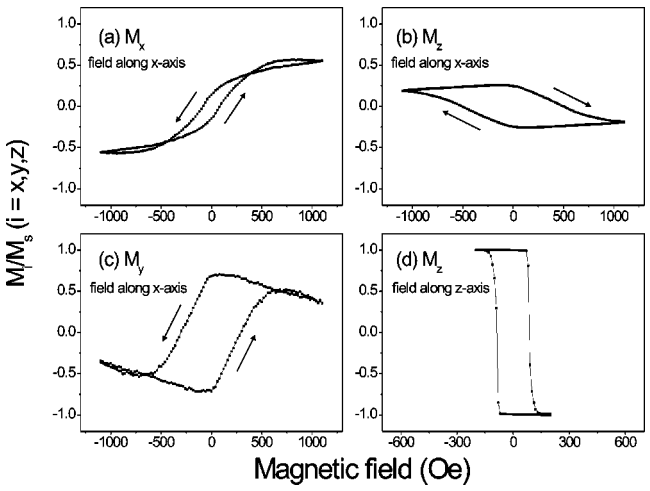

FIG. 8. (a)–(c) are the normalized magnetization components versus the in-plane field. The same scaling factors as in Fig. 4 are used for the normalization. The film thickness (5.3 ± 0.3 ML) was chosen to be within the spin-reorientation transition. The arrows indicate the switching directions. (d) is the hysteresis loop obtained in a vertical field.

factors. Any shift of the data points in the individual components can be ruled out as the Kerr signals in both MOKE setups are obtained at the same time in the same field and the calculation is made point by point. Furthermore, we performed a cross-check by shifting the data points one point upward or downward. The result is the same, i.e., the two dips still remain in the plot. To exclude also an effect due to the uncertainty of the calibration factors, we made a worst-case estimation. With 10% error margin we obtain in the plot a 20% effect, which cannot explain the strong decrease of around 60%. Hence, we have to assign the finding to the magnetic behavior of the sample. The strong decrease is most likely due to the creation of domains and the movement of domain walls. In case of coherent rotation of a single domain state the signal should stay constant everywhere. The single domain configuration splits up into a multidomain state in a field range where the reversal takes place. As the switching of the magnetization via domain nucleation and domain-wall movement can happen within a small field range our data are not dense enough to resolve the whole process in more detail. Consequently, we find only the trace of such a process, i.e., a loss of magnetization signal.

There are three generic cases of SRT for a uniaxial anisotropy system in second-order anisotropy approximation according to the sign of the second-order anisotropy constant K_2 within the transition.[32] The transition from the out-of-plane magnetization to the in-plane magnetization may happen via continuous canting of magnetization when $K_2 > 0$, or it directly changes from the vertical to the in-plane direction when $K_2 = 0$. The third situation appears when $K_2 < 0$, where the transition proceeds via a state of coexisting phases.

For the Co-on-Au(111) system two opposing results are reported. Allenspach *et al.*[17] claimed to find a canting of magnetization in the SRT while Oepen *et al.*[33,34] found evidence for a SRT via a state of coexisting phases. The essential difference between these two states is that the free energy in zero field has only one minimum at a certain canting angle in the first case while in the latter case two local minima for the vertical and the in-plane directions exist. Hence, only in case of coexisting phases the magnetization in zero field can be stabilized in one of these two special directions, i.e., the vertical or the in-plane direction.

To further identify the spin-reorientation transition of Co film on Au(111), we have also taken hysteresis loops at a thickness just within the spin-reorientation transition, i.e. at 5.3 ± 0.3 ML. In Figs. 8(a)–(c) the normalized individual components of magnetization in an in-plane field are shown using the sensitivities determined above. In all three components we find remanence and nonvanishing signals even at 1100 Oe. For M_x the remanence is lower than the signal in high field while the other two components reveal an opposite behavior. The remanence is found in both vertical and in-plane directions, which indicates that the thickness is indeed within the spin-reorientation transition. Taking an in-plane anisotropy into account, it is not surprising to find the maximum remanence in the *y* direction, which is around 80% of the full magnetization. Obviously, the in-plane easy axis is closer to the *y* direction.

The absolute value of the magnetization vector versus the applied field is shown in Fig. 9. We find minima around ± 250 Oe that indicate that the dominant switching behavior is via domain-wall movement. It is somewhat strange that the magnetization signal decreases with increasing field above 500 Oe since an external field should drive the magnetization into a single domain state. To exclude the experimental error, we took the above-mentioned error margins of the scaling factors and recalculated the absolute magnetization value. We find that the magnetization signal still decreases with increasing field above 500 Oe within our experimental uncertainties. Hence, we have to consider it as a true magnetic behavior. The effect could be understood as follows. Although the magnetization has been switched by the external field, the field strength is still not large enough to erase all domains, which becomes evident from the fact that $\sqrt{(M/M_S)^2} < 1$. The remaining domains are not strictly parallel/antiparallel to the field direction as magnetization signals are found in the other two directions as well. Besides

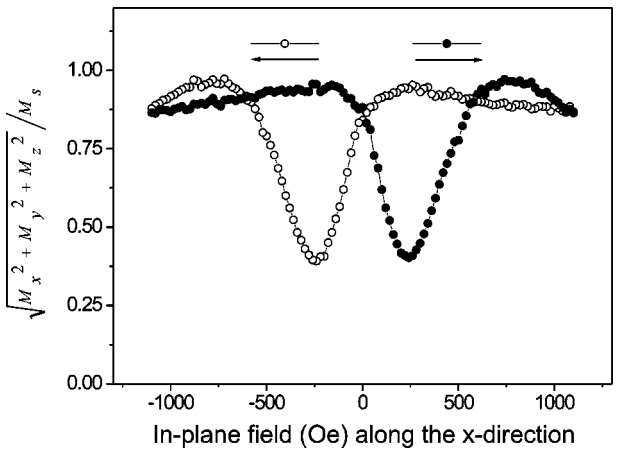

FIG. 9. The value of the magnetization calculated from the individual components in Fig. 8.

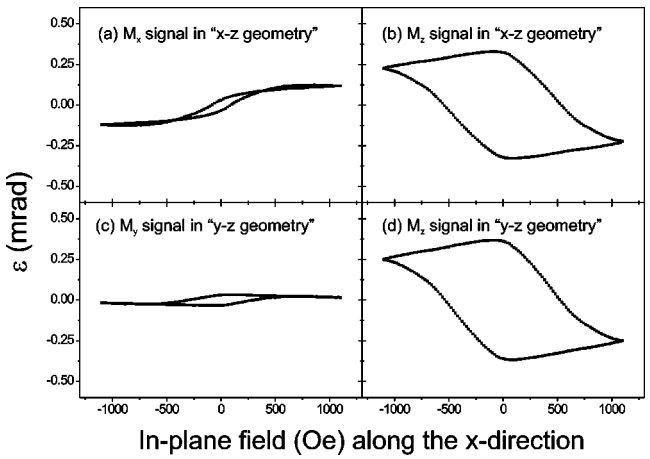

FIG. 10. The original data used for calculating the data shown in Figs. 8 and 9.

this canting of the magnetization of such domains, nucleation of domains and propagation of domain walls has to be expected. The decrease of magnetization value (in Fig. 9) could be due to the changes in the population of the different domains. The value obtained at $|H| \geqslant 1000$ Oe is nearly constant when reducing the field. This indicates that magnetization rotation is the dominant process until the flipping starts. Increasing the field in the opposite direction results in a flipping mainly in the *y* direction continued by an irreversible change in domain population. In order to demonstrate that no uncertainties of the experiments are responsible for the effects seen in Fig. 9 we plotted the original data in Fig. 10. In Figs. 10(a) and (b) are Kerr ellipticities along the *x* and *z* directions obtained in the ''*x*-*z* geometry.'' The Kerr ellipticities along the *y* and *z* direction obtained in the ''*y*-*z* geometry'' are plotted in Figs. 10(c) and (d). We find that the Kerr ellipticities along the *z* direction obtained by two measurements in different geometries are the same, within an error margin of less than 10%.

For a state of magnetization in canting or coexisting phases one would expect remanence in the vertical as well as the in-plane direction. Applying a field in different directions should help to distinguish between these two scenarios of spin-reorientation transition. In a case of canting magnetization the vertical component of magnetization should show a value in remanence that is independent of the field direction as there is only one free-energy minimum. On the other hand, for coexisting phases the value obtained in remanence depends on the direction along which the field has been applied.

In a vertical field we obtained a polar loop with full remanence, i.e., $M_r/M_s = 1$ [see Fig. 8(d)]. The saturation value of the signal 1340 ± 25 μrad is in complete agreement with the value obtained from the thickness dependence of the polar signal in saturation.[35] Apparently, the magnetization stays in perpendicular direction with a single domain state at zero field after saturating the film in a vertical field. This is strong proof for the transition to proceed via a state of coexisting phases instead of a canting state, since full remanence in the vertical direction can only be found in case of a state of coexisting phases within the spin-reorientation transition. Evidence for coexisting phases within the spin-reorientation transition was recently found for Fe/Cu(001) as well.[36]

V. CONCLUSIONS

In summary, we have developed a method to obtain the individual components of magnetization by means of a three-dimensional-MOKE technique. We applied this method to study the spin-reorientation transition of Co films on Au(111). Below the spin-reorientation transition, we observed a square loop in a vertical field, while in an in-plane field the magnetization has components not only along the field direction but also in perpendicular direction, which is attributed to a small misalignment of the field. Beyond the spin-reorientation transition, i.e., with an in-plane easy axis, we observe a hard axis loop in vertical field. The film is almost saturated in the film plane with a maximum in-plane field of 1100 Oe. The hysteresis indicates that there is domain nucleation during the reversal process. Within the transition region, the magnetization has remanence and nonvanishing components in all three directions in an in-plane field. After saturating the film in a vertical field, the magnetization remains in perpendicular direction with full remanence. From that behavior we conclude that the spin-reorientation transition of Co on Au(111) proceeds via a state of coexisting phases and not via continuous magnetization canting.

*Present address: Institut für Angewandte Physik, Universität Hamburg, Jungiusstrasse 11, 20335, Hamburg, Germany.
†Email address: oepen@physnet.uni-hamburg.de

[1] U. Admon, M.P. Dariel, E. Grunbaum, and J.C. Lodder, J. Appl. Phys. **66**, 316 (1989).
[2] E.M. Bradley and M. Prutton, J. Electron. Control **6**, 81 (1959).
[3] C.D. Olson and A.V. Pohm, J. Appl. Phys. **29**, 274 (1958).
[4] S.D. Bader, J. Magn. Magn. Mater. **100**, 440 (1991), and references therein.
[5] S.D. Bader and J.L. Erskine, in *Ultrathin Magnetic Structures*, edited by J.A.C. Bland and B. Heinrich (Springer-Verlag, Berlin, 1994), Vol. II, Chap. 4, and references therein.

[6] A. Hubert and R. Schäfer, *Magnetic Domains* (Springer-Verlag, Berlin, 1998), Chap. 2 and 3, and references therein.
[7] J.M. Florczak and E. Dan Dahlberg, J. Appl. Phys. **67**, 7520 (1990); Phys. Rev. B **44**, 9338 (1991).
[8] C. Daboo, J.A.C. Bland, R.J. Hicken, A.J.R. Ivews, and M.J. Baird, Phys. Rev. B **47**, 11 852 (1993).
[9] W. Rave, R. Schäfer, and A. Hubert, J. Magn. Magn. Mater. **65**, 7 (1987).
[10] P. Büscher and L. Reimer, Scanning **15**, 123 (1993).
[11] S.M. Jordan and J.S.S. Whiting, Rev. Sci. Instrum. **6**, 4286 (1996); J. Magn. Magn. Mater. **172**, 69 (1997).
[12] Z.J. Yang and M.R. Scheinfein, J. Appl. Phys. **74**, 6810 (1993).
[13] Z.Q. Qiu, J. Pearson, and S.D. Bader, Phys. Rev. Lett. **70**, 1006 (1993).
[14] A. Berger and M.R. Pufall, J. Appl. Phys. **85**, 4583 (1999).
[15] H.F. Ding, S. Pütter, H.P. Oepen, and J. Kirschner, J. Magn. Magn. Mater. **212**, L5 (2000).
[16] C. Chappert, D. Renard, P. Beauvillain, J.P. Renard, and J. Seiden, J. Magn. Magn. Mater. **54-57**, 795 (1986).
[17] R. Allenspach, M. Stampanoni, and A. Bischof, Phys. Rev. Lett. **65**, 3344 (1990).
[18] R.P. Hunt, J. Appl. Phys. **38**, 1652 (1967).
[19] M.J. Freiser, IEEE Trans. Magn. **4**, 152 (1968).
[20] J. Zak, E.R. Moog, C. Liu, and S.D. Bader, J. Magn. Magn. Mater. **89**, 107 (1990); J. Appl. Phys. **68**, 4203 (1990); Phys. Rev. B **43**, 6423 (1991).
[21] C.-Y. You and S.-C. Shin, Appl. Phys. Lett. **69**, 1315 (1996).
[22] In this paper, we define the angle of incidence as positive when the incident beam is closer to the positive component of magnetization effective in the longitudinal Kerr effect.
[23] D.M. Zehner and J.F. Wendelken, in *Proceedings of the Seventh International Vacuum Congr. and Third International Conference on Solid Surfaces, Vienna, 1977*, edited by R. Dobrozemsky *et al.* (Berger, Vienna, 1977), p. 517.
[24] W.J. Kaiser and R.C. Jaklevic, Surf. Sci. Lett. **182**, L227 (1987).
[25] M. Speckmann, H.P. Oepen, and H. Ibach, Phys. Rev. Lett. **75**, 2035 (1995).
[26] A misalignment of a few degrees has to be expected.
[27] E.R. Moog, C. Liu, S.D. Bader, and J. Zak, Phys. Rev. B **39**, 6949 (1989).
[28] Z.Q. Qiu, J. Pearson, and S.D. Bader, Phys. Rev. B **46**, 8195 (1992).
[29] R.M. Osgood III, K.T. Riggs, A.E. Johnson, J.E. Mattson, C.H. Sowers, and S.D. Bader, Phys. Rev. B **56**, 2627 (1997).
[30] *CRC Handbook of Chemistry and Physics*, 74th ed. (CRC Press, Boca Raton, FL, 1993).
[31] Generally speaking, it is not necessary to calculate the longitudinal Kerr-effect sensitivities if the angles of incidence in both geometries are the same.
[32] Y.T. Millev and J. Kirschner, Phys. Rev. B **54**, 4137 (1996).
[33] H.P. Oepen, M. Speckmann, Y.T. Millev, and J. Kirschner, Phys. Rev. B **55**, 2752 (1997).
[34] H.P. Oepen, Y.T. Millev, and J. Kirschner, J. Appl. Phys. **81**, 5044 (1997).
[35] S. Pütter, Ph.D. thesis, Martin-Luther University, 2000.
[36] E. Mentz, A. Bauer, T. Günther, and G. Kaindl, Phys. Rev. B **60**, 7379 (1999).